BULLETIN OF THE POLISH ACADEMY OF SCIENCES
TECHNICAL SCIENCES, Vol. 68, No. 2, 2020
DOI: 10.24425/bpasts.2020.133122

Thermo-, magneto- and photo- dependent electrical properties of hierarchical *InSe<β-CD<FeSO$_4$>>* supramolecular compound

T. POPŁAWSKI[1], I. BORDUN[1]*, and A. PIDLUZHNA[2]

[1] Czestochowa University of Technology, Al. Armii Krajowej 17, Czestochowa, 42-200, Poland,
[2] Lviv Polytechnic National University, Bandera Str. 12, Lviv, 79013, Ukraine

Abstract. The hierarchical structure of *InSe<β-CD<FeSO$_4$>>* composition with 4-fold grade expansion was synthesized with the intercalation-deintercalation technique. Electrical properties of the structure obtained were examined using impedance and thermostimulated current spectroscopy methods. Influence of temperature, static magnetic field and illumination on electrical properties of the synthesized compound was investigated. Changes in the impurity spectrum of the expanded hierarchical structure were analyzed and extraordinary magneto- and photoimpedance behavior of *InSe<β-CD<FeSO$_4$>>* at room temperature was explained.

Key words: impedance analysis, *InSe*, *β*-cyclodextrin, photoresistive effect, magnetoresistive effect.

1. Introduction

Supramolecular chemistry has been the object of great interest in the scientific world during in recent decades [1–4]. Certainly massive progress in this field is accompanied by multiple articles devoted to investigation of different properties of supramolecular compounds in general, and clathrates in particular. Among them, a list of works addressing photosensible and conductive properties of supramolecular compounds proves closest to practical application in the nanoelectronics area [5–9]. For example, the Slack hypothesis [10, 11] was proved experimentally when structures with weakly bonded atoms, which can oscillate in confined space providing poor thermal conductivity with good electric conductivity, were successfully formed [12]. A variety of works deals with other physical aspects of supramolecular structures, and works on theoretic electron structure calculations [13] and systems with exciton energy transfer [14] are worth noting among others.

In a recent work [15], our colleagues described the synthesis of principally new supramolecular subhost<host<guest>> clathrate ensemble with SiO_2 based MCM-41 as subhost matrix for *β*-cyclodextrin (*β-CD*) as a host and iron (II) sulfate (*FeSO$_4$*) as a guest component. Giant magneto-capacitive and alternating current negative magneto-capacitive effects were discovered in the synthesized structure at room temperature, with weak magnetic field and in the $10^3 \div 10^6$ Hz frequency region. Such peculiar properties of hierarchical clathrates are of tremendous interest obviously because there is great interest in novel materials for nanophotoelectronic and quantum coherent spintronic applications [16–22]. Therefore this work deals with investigation of thermo-, magneto- and photo- dependent electric properties of hierarchical structure based on photosensitive semiconductive and quasi 2D Indium Selenide *InSe* as the subhost material and *β-CD* as a host and *FeSO$_4$* as a guest component.

It should be mentioned that together with colleagues from our research group we have synthesized *InSe<β-CD<FeSO$_4$>>*. One part of this sample was used by our colleagues to compare properties of the obtained substance with a similar one but synthesized under lighting and electric field, and results were discussed and published [23]. The task of the present work was to investigate the electrical properties of hierarchical clathrate with different quantity *Q* of *<β-CD<FeSO$_4$>>$_Q$* of the <host<guest>> component under normal conditions and under illumination, magnetic field and continuous heating.

2. Methods and experiments

Monocrystalline *InSe* as the subhost structure was used for hierarchical *InSe<β-CD<FeSO$_4$>>$_Q$* clathrate synthesis. The compound was formed by means of the intercalation method, i.e. the insertion of ions, atoms or molecules into intracrystalline cavities [24]. It is described in [23].

InSe monocrystal with definite layer structure and n-type conductivity was grown by the Bridgman–Stockbarger technique. The optical band gap of the material is 1.2 eV [25]. The *InSe* layered crystal forms guest positions are oriented perpendicularly to crystallographic C axis [26] within the plane of weak Van der Waals interaction. The lack of dangling bonds at the surface provides very low surface recombination speed. Furthermore, *InSe* monocrystal is very photosensitive within the visible range of the specter.

Organic *β*-cyclodextrin $C_{42}H_{70}O_{35}$ (*β-CD*) was used as the host component. The structural particular feature of the compound such as spatial separation of hydrophilic and hydrophobic groups determines its physical and chemical properties. The most

*e-mail: ihor.bordun@pcz.pl

Manuscript submitted 2019-03-07, revised 2019-10-04, initially accepted for publication 2019-12-01, published in April 2020

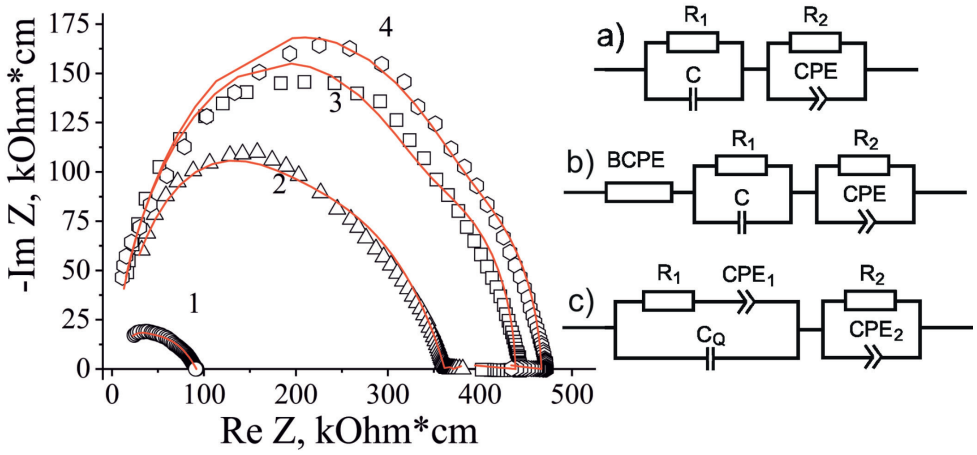

Fig. 1. Nyquist diagrams of initial expanded *InSe* matrix (plot 1) and of *InSe*<*β-CD*<$FeSO_4$>>$_Q$ measured at room temperature in darkness and perpendicularly to nanolayers for Q = 5 wt% (plot 2), Q = 11 wt% (plot 3) and Q = 17 wt% (plot 4). Inset contains equivalent electrical schemes for initial InSe matrix – a, for Q = 5 wt% – b, Q = 11 and 17 wt% – c

important feature among them is the ability to bind organic, inorganic and biological molecules selectively and reversibly and form insertion complexes with the lock and key model. The high electron density of the *β-CD* intracavitary region can activate electrons of guest molecules, which results in spectral properties change of both inserted molecules and *β-CD* [1, 27].

Iron (II) sulfate $FeSO_4$ was chosen as the guest component. It is well-known as a precursor for nanomagnetite synthesis with a cation which possesses high spin magnetic momentum.

Since neither *β-CD* nor $FeSO_4$ can be inserted into *InSe* directly, the supramolecular ensemble formation was executed by means of three stage intercalation-deintercalation technique [28]. The initial *InSe* matrix was expanded in 4-fold grade with this technique. The gain in quantity of the host<guest> component in the expanded *InSe* matrix was reached in a stepwise intercalation procedure with precise measuring at every step.

Impedance measurements were performed along crystallographic C axis direction in the $10^{-3} \div 10^{6}$ Hz frequency region using the Autolab PGSTAT10 potentiostat-galvanostat (Eco-Chemie) with FRA2 and GPES modules installed. Frequency dependences of complex impedance Z were evaluated with the method of graph analysis with Dirichlet filter [28, 29] in ZView2.3 software environment (Scribner Associates). Errors of approximation did not override the value of 4%. Adequacy of proposed impedance models in respect to experimental data was confirmed by the completely random character of frequency dependence of 1-order residual differences [29, 30]. Impedance measurements were also carried out in static magnetic field (magnetic field strength 2.75 kOe) and under illumination (solar simulator 65 W) along crystallographic C axis. Such a geometry was chosen to minimize the Lorentz force component.

3. Results and discussion

3.1. Impedance analysis of synthesized hierarchical *InSe*<*β-CD*<$FeSO_4$>>$_Q$. Impedance spectra of *InSe*<*β-CD*<$FeSO_4$>>$_Q$ and initial *InSe* matrix are presented in Fig. 1. Presence of trap centers in the neighborhood of Fermi level and charge carriers jumps on it determine substantial contribution to *ac* electric conductivity. Therefore the transformation of a point as an impedance image of a lumped reactance element in a complex impedance plane into hodograph plot is observed. The Nyquist plot of expanded *InSe* matrix is of *ex ante* character with superposition of two semicircles.

The first high frequency semicircle represents the process of free current flow of intercalant packages of layers and the second low frequency part reflects charge transfer between packages. The equivalent electric scheme for this case is presented in inset *a* of Fig. 1.

Impedance spectra Z(ω) of initial expanded *InSe* matrix (Fig. 1, plot 1) and of *InSe*<*β-CD*<$FeSO_4$>>$_Q$ in Nyquist diagram form are measured at room temperature in darkness and perpendicularly to nanolayers for $Q = 5$ *wt*% (Fig. 1, plot 2), $Q = 11$ *wt*% (Fig. 1, plot 3) and $Q = 17$ *wt*% (Fig. 1, plot 4).

Parallel high frequency R_1/C chain link is equivalent to current flow in unexpanded packages of matrix layers with localized states in the neighborhood of the Fermi level. The low frequency R_2/CPE chain link reflects the interpackage charge transfer. CPE is the constant phase element of capacitive nature [29] which models the distributed capacity caused by presence of vacancies or impurity states. Both of them provide electron conductivity at room temperature.

The Nyquist plot for synthesized hierarchical compound changes drastically in value for real and imaginary parts of complex impedance and for its hodograph in the low frequency region as well. Above all, it is a change into frequency-independent character in the low frequency region for $Q = 5$ *wt*% and simultaneous frequency inversion with <host<guest>> component increase for $Q = 11$ to 17 *wt*%. In the first case, for $Q = 5$ *wt*%, the low frequency horizontal plot is modeled by the BCPE (bounded constant phase element) chain link, which represents current flow in a spatially limited area with complex conductivity [29]. The behavior of the real part of complex

impedance ReZ(f) for samples with $Q = 11$ and 17 *wt*% of *β-CD<FeSO₄>* component becomes extraordinary in the low frequency region. Arising from zone carriers, conductivity follows down with an increase in frequency. This type of behavior evidences demonstration of the Luryi quantum capacitance C_Q [31] effect in sampled states perpendicular to nanolayers. This capacity is placed in parallel to the serial R_1 CPE chain link (Fig.1 *c*).

In this case, the shift of maximum positions for imaginary part of complex impedance – ImZ(ω) (Fig. 2) after intercalation of *β-CD<FeSO₄>* into *InSe* was expected because of change in impurity electron subband, and consequent deep trap centers infusion.

However, more importantly, the low frequency inversion of hodograph plots (Fig. 1, plots 3–4) is relative to maxima shift for –ImZ(ω) for *InSe<β-CD<FeSO₄>>*$_Q$ in the region of $1.9*10^5$ Hz to $6.3*10^4$ Hz (Fig. 2).

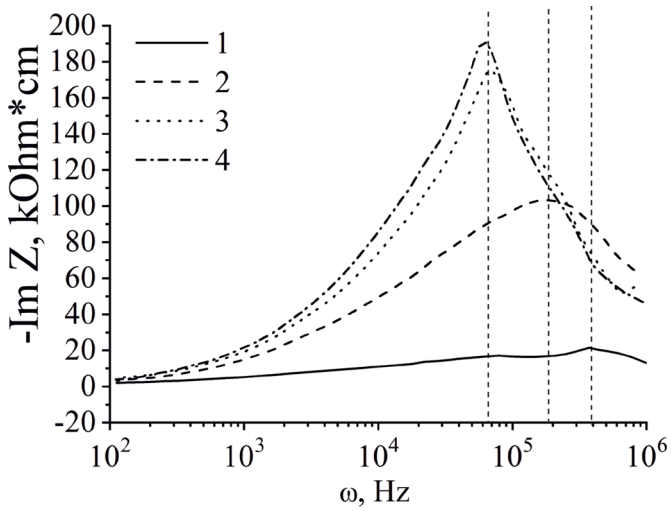

Fig. 2. Frequency ω dependent imaginary term of complex impedance –ImZ(ω) of initial expanded *InSe* matrix (plot 1) and of *InSe<β-CD<FeSO₄>>*$_Q$ measured at room temperature in darkness and perpendicularly to nanolayers for Q = 5 wt% (plot 2), Q = 11 wt% (plot 3) and Q = 17 wt% (plot 4)

3.2. Investigation of impurity subsystem of synthesized *InSe<β-CD<FeSO₄>>*$_Q$ by using thermoelectric technique. The spectra of thermostimulated currents were measured to confirm the change in energy topology of the impurity band in the neighborhood of the Fermi level. Spectra are plotted in Fig. 3. They validate the transformation of energy topology spectra from practically quasicontinuous ones to the band spectrum for Q = 5, 11 and 17 *wt*%.

Hence, the structure of *InSe* with the *β-CD<FeSO₄>*component of $Q = 5$ *wt*% quantity represents the system of coordination defects with a structure other than the one of initial matrix and with negative correlation energy. This system forms a quasicontinuous spectrum of localized states in a band gap. Spectra of thermostimulated current for samples with $Q = 11$ and 17 *wt*% transform into narrow bands with essentially higher

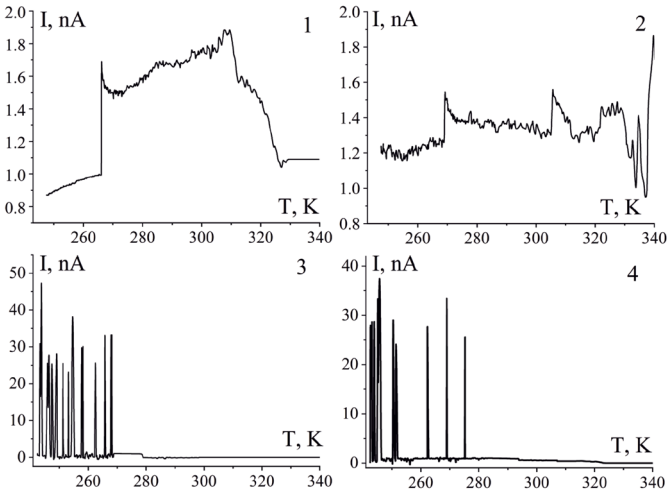

Fig. 3. Thermostimulated current spectra of initial expanded *InSe* matrix (1) and of *InSe<β-CD<FeSO₄>>*$_Q$ for $Q = 5$ *wt*% (2), $Q = 11$ *wt*% (3) and $Q = 17$ *wt*% (4)

density of states and well-marked miniband character. Calculation results for the impurity energy spectrum according to the Geballe-Pollak theory [32–34] are presented in Fig. 4a.

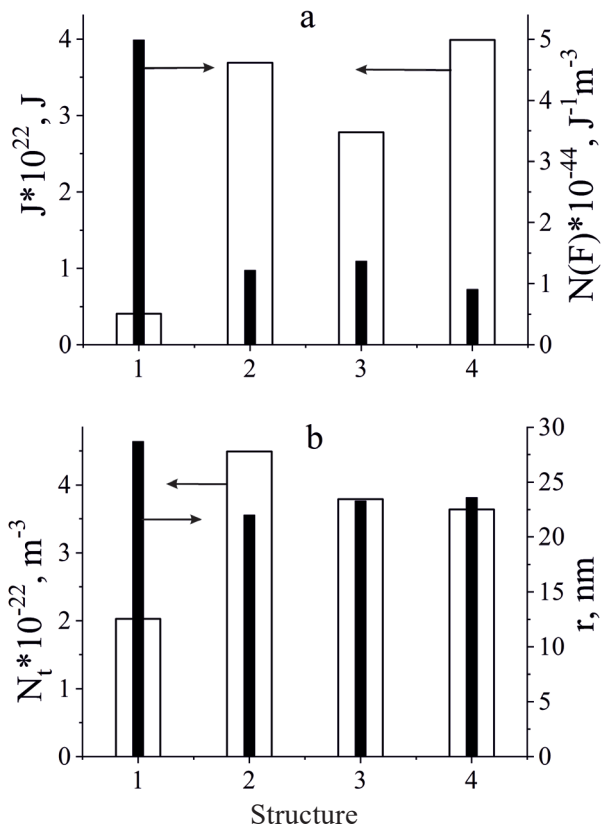

Fig. 4. Trap centers dispersion *J* (a), density of states at Fermi level *N*(*F*) (a), real density of deep traps N_t (b) and jump distance *r* (b) in *InSe<β-CD<FeSO₄>>*$_Q$ for initial *InSe* matrix (structure 1), $Q = 5$ *wt*% (structure 2), $Q = 11$ *wt*% (structure 3) and $Q = 17$ *wt*% (structure 4)

Intercalation of the <host<guest>> component for $Q = 5$ *wt*% (structure 2, Fig. 4a) results in 4-fold decrease in trap centers dispersion J and 7-fold increase in the density of states at the Fermi level $N(F)$. Further intercalation $Q = 11$ *wt*% (structure 3, Fig. 4a) leads to nonmonotonic changes in the above-listed parameters. The changes were also observed for real density of deep traps N_t and jump distance r (Fig. 4b). In the first case, the intercalation of β-CD<$FeSO_4$> into *InSe* results in an over 2-fold increase in N_t and in the second case – in a slight decrease in r. Monotonic decrease N_t and increase r were observed for samples from $Q = 5$ to 17 *wt*% (structure 2–4, Fig. 4b).

3.3. Impedance analysis of synthesized hierarchical *InSe*<*β-CD*<*FeSO*$_4$>>$_Q$ under magnetic field and illumination. Considering the physical properties of guest β-CD [1, 27] and $FeSO_4$ components and the corresponding change in the impurity electron subsystem for *InSe*<β-CD<$FeSO_4$>>$_Q$, it was important to investigate the external physical field effect on conductive and polarization properties of the synthesized hierarchical structure. With this purpose, impedance analysis for *InSe*<β-CD<$FeSO_4$>>$_Q$ with magnetic field applied and with illumination was carried out. As it was determined, the influence of static magnetic field is not remarkable by the value but it proves essential in relation to frequency dispersion of the real component of complex impedance. The medium frequency oscillations became noticeable for *InSe*<β-CD<$FeSO_4$>>$_Q$ for $Q = 11$ and 17 *wt*% (Fig. 5) under the static magnetic field applied.

The reason for such oscillation is connected to the impurity spectrum modification by means of quantum amplification with guest content of Zeeman splitting [35]. This assumption was confirmed by the band spectrum for thermostimulated current for samples with $Q = 11$ and 17 *wt*% (Fig. 3) in contrast to the quasimonotonous spectrum for $Q = 5$ *wt*%.

The intercalation of β-CD<$FeSO_4$> into *InSe* leads to a 4-fold increase in photosensitivity of resulting hierarchical clathrate. However, the specific feature of response of nanostructure to illumination is the formation of low frequency oscillations of real part of complex impedance (Fig. 5). In contrast to the magnetic field case, oscillations at illumination are inherent in all three samples of clathrate and are caused by the negative capacitance effect.

This effect is well-known [36, 37] and explained in detail [38, 39] for the class of compounds that the present work deals with.

Such interest in clathrate compounds based on semiconductive host matrixes developed owing to possibility of their application in nanoelectronics for formation of integrator free delay nanolines. But the specific character of the present case consists in visualization of changes under illumination, which means the onset of photoinduced negative capacitance. The mechanism of the observed effect involves photoexcitation of electrons from occupied states below the Fermi level and formation of trap centers for injected electrons with relaxation time longer than the half-cycle of sinusoidal signal. The Nyqist plots for the clathrates being investigated (Fig. 6) evidence the above-stated assumption. Impedance spectra indeed include fragments in the IV-inductive quadrant of a complex plane, and can be modeled by circuits with inductive element L (inset in Fig. 6). Therefore practical importance of the effect obtained deserves consideration for formation of delay nanolines controlled optically.

The values for magneto- χ and photoresistive ξ effects were calculated using the following formulas, respectively:

$$\chi = \frac{\rho(H) - \rho(0)}{\rho(0)}, \tag{1}$$

$$\xi = \frac{\rho(dark) - \rho(light)}{\rho(light)}, \tag{2}$$

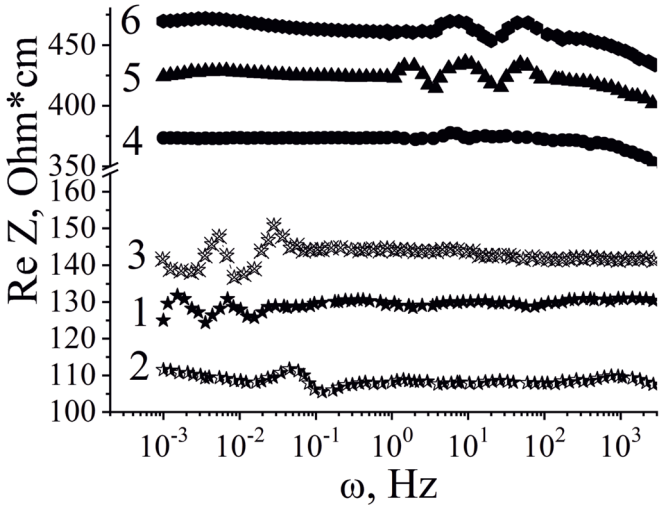

Fig. 5. Frequency-dependent real term of complex impedance *ReZ* of *InSe*<β-CD<$FeSO_4$>>$_Q$ measured at room temperature perpendicularly to nanolayers for $Q = 5$ *wt*% (1, 4), $Q = 11$ *wt*% (2, 5) and $Q = 17$ *wt*% (3, 6). Measurements carried out with illumination (1–3) and with magnetic field applied (4–6)

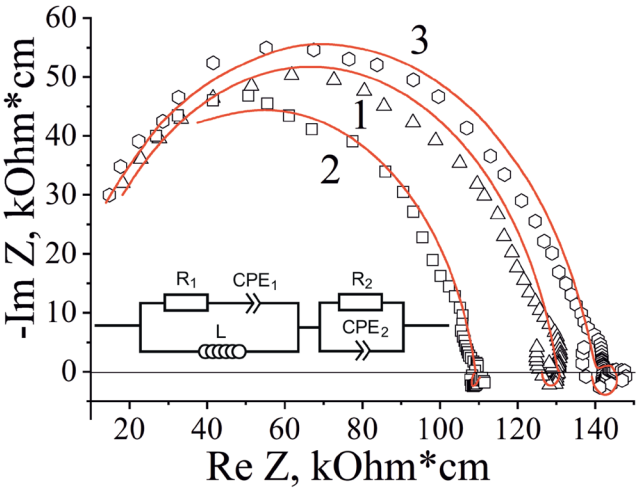

Fig. 6. Nyquist plots for *InSe*<β-CD<$FeSO_4$>>$_Q$ compound measured at room temperature and with illumination perpendicularly to nanolayers for $Q = 5$ *wt*% (1), $Q = 11$ *wt*% (2) and $Q = 17$ *wt*% (3). Measured values of complex impedance Z for investigated samples plotted in symbols and results of modeling presented as lines. Inset contains equivalent electrical scheme for impedance hodographs

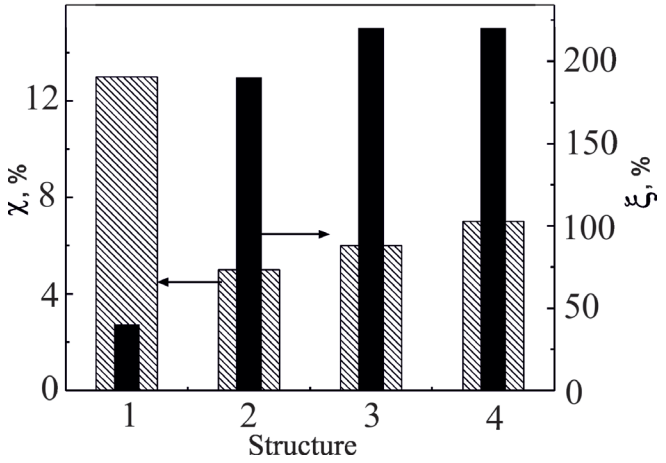

Fig. 7. Magneto- χ and photo- ξ resistive effects of $InSe<\beta\text{-}CD<FeSO_4>>_Q$ compound measured at room temperature and with illumination perpendicularly to nanolayers for initial *InSe* matrix (structure 1), $Q = 5$ *wt*% (structure 2), $Q = 11$ *wt*% (structure 3) and $Q = 17$ *wt*% (structure 4)

and are presented in Fig. 7. Here $\rho(H)$ is resistance measured in the magnetic field applied, $\rho(0)$ is resistance measured under normal conditions, $\rho(dark)$ is resistance measured in the dark and $\rho(light)$ is resistance measured at impressed illumination.

The values of photoresistive effect obtained confirm the potential of formation of highly sensible photovaricaps based on $InSe<\beta\text{-}CD<FeSO_4>>_Q$ structures.

4. Conclusions

In conclusion, the hierarchical clathrate multilayered structure of composition $InSe<\beta\text{-}CD<FeSO_4>>_Q$ was synthesized successfully. As it was shown, the quantity Q of the guest component essentially determines the behavior of the compound physical properties and electron energy structure.

Quantum capacitance contributes substantially to the current flow for synthesized $InSe<\beta\text{-}CD<FeSO_4>>_Q$ with $Q = 11$ and 17 *wt*% only.

The static magnetic field applied evokes ReZ(f) oscillations in the middle frequency region. The reason for oscillation of real term of complex impedance is caused by impurity spectrum modification due to quantum boost with guest content of Zeeman splitting. The effect described is observed in $InSe<\beta\text{-}CD<<FeSO_4>>_Q$ clathrates with $Q = 11$ and 17 *wt*%. They are characterized by band spectrum with essentially higher density of states and clearly defined miniband character.

The effect of negative capacitance was registered for all samples of $InSe<\beta\text{-}CD<FeSO_4>>_Q$ regardless of guest quantity Q and is induced by illumination. The intercalation of hierarchical guest $\beta\text{-}CD<FeSO_4>$ into 4-fold expanded *InSe* matrix leads to 4-fold increase in photosensitivity of the obtained $InSe<\beta\text{-}CD<FeSO_4>>_Q$ compound and photoresistance for samples with Q = 5, 11 and 17 *wt*% takes the value of 185, 200 and 200%, respectively.

The described effect renders synthesized structures attractive samples for the formation of delay nanolines controlled optically.

References

[1] *Analytical Methods in Supramolecular Chemistry*, ed. C.A. Schalley, WILEY-VCH Verlag GmbH & Co. KGaA, Weinheim, 2007.

[2] S. van der Zwaag, "Routes and mechanisms towards self healing behavior in engineering materials", *Bull. Pol. Ac.: Tech.* 58(2), 227–236 (2010).

[3] J. Murray, K. Kim, T. Ogoshi, W. Yao, and B.C. Gibb, "The aqueous supramolecular chemistry of cucurbit[n]urils, pillar[n] arenes and deep-cavity cavitands", *Chem.Soc.Rev.* 46, 2479–2496 (2017).

[4] D. Gontero, M. Lessard-Viger, D. Brouard, A.G. Bracamonte, D. Boudreau, and A.V. Veglia, "Smart multifunctional nanoparticles design as sensors and drug delivery systems based on supramolecular chemistry", *Microchem. Journal* 130, 316–328 (2017).

[5] H. Masai and J. Terao, "Stimuli-responsive functionalized insulated conjugated polymers", *Polymer Journal* 49, 805–814 (2017).

[6] Y. Takashima and A. Harada, "Stimuli-responsive polymeric materials functioning via host–guest interactions", *J. Incl. Phenom. Macrocycl. Chem.* 88(3–4), 85–104 (2017).

[7] F. Yuen and K. C. Tam, "Cyclodextrin-assisted assembly of stimuli-responsive polymers in aqueous media", *Soft Matter.* 6(19), 4613–4630, (2010).

[8] Q. He, P. Tu, and J.L. Sessler, "Supramolecular Chemistry of Anionic Dimers, Trimers, Tetramers, and Clusters", *Chem.* 4(1), 46–93, (2018).

[9] L. Wang and Q. Li, "Photochromism into nanosystems: towards lighting up the future nanoworld", *Chem. Soc. Rev.* 47(3), 1044–1097 (2018).

[10] M. Baroncini, L. Casimiro, C. de Vet, J. Groppi, S. Silvi and A. Credi, "Making and Operating Molecular Machines: A Multidisciplinary Challenge", *ChemistryOpen* 7(2), 169–179 (2018).

[11] G.A. Slack, "Design concepts for improved thermoelectric materials", in *Mat. Res. Soc. Symp. Proc.*, vol. 478, pp 47–54, eds. T.M. Tritt, M.G. Kanatzidis, H.B. Lyon and G.D. Mahan, MRS Press, Warrendale, Pennsylvania, 1997.

[12] A.V. Shevelkov, E.A. Kelm, A.V. Olenev, V.A. Kulbachinskii, and V.G. Kytin, "Anomalously low thermal conductivity and thermoelectric properties of new cationic clathrates in the Sn-In-As-I system", *Semiconductors* 45(11), 1399–1403 (2011).

[13] N.A. Borshch, N.S. Pereslavtseva, and S.I. Kurganskii, "Electronic structure of Zn-substituted germanium clathrates", *Semiconductors* 43(5), 563–567 (2009).

[14] M.S. Ibrahim and S. El-din H. Etaiw, "Supramolecular host–guest systems as frameworks for excitation energy transfer", *Spectrochimica Acta., Part A: Molecular and Biomolecular Spectroscopy* 58 (2), 373–378 (2002).

[15] T.M. Bishchaniuk and I.I. Grygorchak "Colossal magnetocapacitance effect at room temperature", *Applied Physics Letters* 104, 203104–1 – 203104–3 (2014).

[16] F.C. Grozema, C. Houarner-Rassin, P. Prins, L.D.A. Siebbeles, and H.L.J. Anderson, "Supramolecular Control of Charge Transport in Molecular Wires", *Am. Chem. Soc.* 129 (44), 13370–13371 (2007).

[17] J.M. Warman, M.P. de Haas, G. Dicker, F.C. Grozema, J. Piris, and M.G. Debije, "Charge Mobilities in Organic Semiconducting Materials Determined by Pulse-Radiolysis Time-Resolved Microwave Conductivity: π-Bond-Conjugated Polymers versus π–π-Stacked Discotics", *Chem. Mater.* 16(23), 4600–4609 (2004).

[18] F.Würthner, Z. Chen, F.J.M. Hoeben, P. Osswald, C.-C. You, P. Jonkheijm, J. van Herrikhuyzen, A.P.H.J. Schenning, P.P.A.M. van der Schoot, E.W. Meijer, E.H.A. Beckers, S.C.J. Meskers, and R.A.J. Janssen, "Supramolecular p−n-Heterojunctions by Co-Self-Organization of Oligo(p-phenylene Vinylene) and Perylene Bisimide Dyes", *J. Am. Chem. Soc.* 126(34), 10611–10618 (2004).

[19] S.X. Xiao, M. Myers, Q. Miao, S. Sanaur, K.L. Pang, M.L. Steigerwald, and C. Nuckolls, "Molecular Wires from Contorted Aromatic Compounds", *Angew. Chem., Int. Ed.* 44 (45), 7390–7394 (2005).

[20] L. Schmidt-Mende, A. Fechtenkötter, K. Müllen, E. Moons, R.H. Friend, and J.D. MacKenzie, "Self-organized discotic liquid crystals for high-efficiency organic photovoltaics", *Science* 293(5532), 1119–1122 (2001).

[21] P.N. Hai, S. Ohya, M. Tanaka, S.E. Barnes, and S. Maekawa, "Electromotive force and huge magnetoresistance in magnetic tunnel junctions", *Nature* 458, 489–492 (2009).

[22] D. Supriyo, "Proposal for a "spin capacitor", *Appl. Phys. Lett.* 87(1), 013115 (2005).

[23] I. Grygorchak, O. Hryhorchak and F. Ivashchyshyn, "Modification of the Properties of InSe⟨b-Cd⟨FeSO4⟩⟩ Clathrate/Cavitate Complexes with Hierarchical Architecture at Their Synthesis in Crossed Electric and Light-Wave Fields", *Ukrainian Journal of Physics* 62(7), 625–632 (2017).

[24] R.M.A. Lies, "III–VI Compounds", in *Preparation and crystal growth material with layered structure*, pp 225–254, ed. R.M.A. Lies, D. Retdel Publishing Company, Dordrecht-Boston, 1977.

[25] R.H. Friend and A.D. Yoffe, "Electronic Properties of intercalation complexes of the transition metal dichalcogenides" *Adv. Phys.* 36(1), 1–94 (1987).

[26] V. Val. Sobolev and V.V. Sobolev, "Optical Properties of Imperfect In_2Se_3", *Semiconductors* 37(7), 757–762 (2003).

[27] E.V. Chernyckh and S.B. Brichkin, "Supramolecular complexes based on cyclodextrins", High Energy *Chemistry* 44(2), 83–100 (2010).

[28] I. Grygorchak, F. Ivashchyshyn, P. Stakhira, R.R. Reghu, V. Cherpak and J.V. Grazulevicius, "Intercalated Nanostructure Consisting of Inorganic Receptor and Organic Ambipolar Semiconductor", *Journal of Nanoelectronics and Optoelectronics* 8(3), 292–296 (2013).

[29] Z. Stoinov, B. Grafov, B. Savvova-Stoinova, and V. Yelkin, *Electrochemical Impedance*, Nauka, Moskow, 1991, [In Russian].

[30] *Impedance spectroscopy. Theory*, *experiment and application*, eds. E. Barsoukov and J.R. Macdonald, Wiley interscience, Hoboken, Jew Jersey, 2005.

[31] S. Luryi, "Quantum capacitance devices", *Appl. Phys. Lett.* 52(6), 501–503 (1988).

[32] I.G. Austin and N.F. Mott, "Polarons in crystalline and non-crystalline materials", *Adv. Phys.* 18(71), 41–102 (1969).

[33] S.K. Lyo and T. Holstein, "Low-Frequency Impurity-Pair Conductivity in Doped Semiconductors", *Phys. Rev. B* 8(2), 682–692 (1973).

[34] T. Holstein, "Hall Effect in Impurity Conduction", *Phys. Rev.* 124, 1329–1347 (1961).

[35] R.V. Demin, L.I. Koroleva, A.Z. Muminov, and Ya.M. Mukovski, "Giant Volume Magnetostriction and Colossal Magnetoresistance in $La_{0.7}Ba_{0.3}MnO_3$ at Room Temperature", *Physics of the Solid State* 48(2), 322–325 (2006).

[36] J. Bisquert, H. Randriamahazaka, and G. Garcia-Belmonte, "Inductive behaviour by charge-transfer and relaxation in solid-state electrochemistry", *Electrochimica Acta*. 51(4), 627–640 (2005).

[37] I. Mora-Sero and J. Bisquert, "Implications of the Negative Capacitance Observed at Forward Bias in Nanocomposite and Polycrystalline Solar Cells", *Nano Letters*. 6(4), 640–650 (2006).

[38] F. Ivashchyshyn, I. Grygorchak, P. Stakhira, V. Cherpak, and M. Micov, "Nonorganic semiconductor – Conductive polymer intercalate nanohybrids: Fabrication, properties, application", *Current Applied Physics*. 12(1), 160–165 (2012).

[39] T.M. Bishchaniuk, I.I. Grygorchak, A.V. Fechan, and F.O. Ivashchyshyn, "Semiconductor clathrates with a periodically modulated topology of a host ferroelectric liquid crystal in thermal, magnetic, and light-wave fields", *Technical Physics* 59(7), 1085–1087 (2014).